Journal of Applied Analysis and Computation
Volume 13, Number 4, August 2023, 1910–1930
Website:http://www.jaac-online.com
DOI:10.11948/20220285

BIFURCATION AND CHAOS ANALYSIS OF A TWO-DIMENSIONAL DISCRETE-TIME PREDATOR–PREY MODEL

Tamer El-Azab[2], M. Y. Hamada[1,2,†] and H. El-Metwally[2]

Abstract The dynamical behavior of a discrete predator–prey system with a nonmonotonic functional response is investigated in this work. We study the local asymptotic stability of the positive equilibrium of the system by examining the characteristic equation of the linearized system corresponding to the model. By choosing the growth rate as a bifurcation parameter, the existence of Neimark-Sacker and period-doubling bifurcations at the positive equilibrium is established. Furthermore, the effects of perturbations on the system dynamics are investigated. Finally, examples are presented to illustrate our main results.

Keywords Discrete predator–prey model, Neimark-Sacker bifurcation, flip bifurcation, center Manifold Theorem.

MSC(2010) 39A10.

1. Introduction

Ecological models show a wide range of non-fixed point dynamics, from simple natural cycles to more complicated chaotic oscillations [2,29]. The study of the predator–prey model is gaining popularity among various ecological models [8]. There are two types of mathematical models in the theory of population dynamical models. The continuous-time models defined by differential equations and the discrete-time models represented by difference equations. Discrete-time population models have gotten a lot of attention in recent years. The causes are as follows: First, when populations have non-overlapping generations or the number of populations is small, discrete-time models are more appropriate than continuous-time models. Second, discrete-time models provide more accurate numerical simulation results. Finally, the discrete-time models have complicated dynamical behaviors; for example bifurcation, chaos, and more complex dynamical behaviors (see, [14,19,21]).

Recently, many authors have studied various characteristics of predator–prey models in detail [3,9,17,18,25]. For example, stability, permanence, and the existence of periodic solutions of predator–prey models are studied in [1,4,7,11–13,20,

†The corresponding author.
Email: Tamerazab@mans.edu.eg(T. El-Azab),
moe_hamada87@hotmail.com(M. Y. Hamada),
Helmetwally@mans.edu.eg(H. El-Metwally)
[1]Mathematics Department, Faculty of Engineering, German International University, Cairo, Egypt
[2]Mathematics Department, Faculty of Science, Mansoura University, Mansoura 35516, Egypt

23, 30, 33]. However, there are few papers that explore the dynamical behavior of predator–prey models, such as bifurcations and chaos occurrences.

The motivation of this paper is to use the theory of difference equations to investigate the behavior of a discrete-time predator-prey model. The construction of this model depends on two main components. The first component, which is the logistic map, is used to represent the growth of the prey. The type III functional response, which is the second component, is utilised to reflect both the interaction between the two species and the growth of the predator. Furthermore, we apply bifurcation theory and the center manifold theorem to construct the conditions of existence for flip bifurcation and Neimark-Sacker bifurcation. The theoretical findings are supported by numerical simulations that show the system's unique and interesting dynamical behavior. More specifically, the period-2, attracting invariant cycles, quasi-periodic orbits, and beautiful chaotic behaviors are presented in this study.

The outline of this paper is as follows: Section 2 investigates the existence of equilibria and local stability of the discrete-time model (2.4) with various topological types. Further, we explore the existence of bifurcations around equilibria. Numerical simulations using MATLAB are applied in Section 5 to support the theoretical analyses and visualize the newly observed complex dynamics of the system. Section 6 contains the conclusion and discussion.

2. Derivation of the Model

We consider a prey–predator model that consists of two constituent populations; i.e., prey and predator. Let $x(t)$ and $y(t)$ denote the population densities of prey and predator at time t, respectively. We impose the following assumptions to formulate the difference equations which describe the model system.

Assumption 2.1. *When predator y is absent, the population of prey x grows in a logistical manner.*

$$x(t+1) = rx(t)\left(1 - x(t)\right). \tag{2.1}$$

Assumption 2.2. *The population of prey x will drop in the presence of the predator y. If we suppose that the interaction between the prey and the predator has a Holling type III functional response due to the prey's defensive ability, equation* (2.1) *can be expressed as*

$$x(t+1) = rx(t)\left(1 - x(t)\right) - \beta\frac{(x(t))^2 y(t)}{(x(t))^2 + 1}.$$

Assumption 2.3. *Prey x are favourite food for predator y, the population density of predator y will increase in a Holling type III functional response manner in the presence of favourite food. Hence we have*

$$y(t+1) = \beta\frac{(x(t))^2 y(t)}{(x(t))^2 + 1}. \tag{2.2}$$

Hence from Eqs. (2.1)-(2.2)

$$\begin{aligned} x(t+1) &= rx(t)\left(1 - x(t)\right) - \beta\frac{(x(t))^2 y(t)}{(x(t))^2 + 1}, \\ y(t+1) &= \beta\frac{(x(t))^2 y(t)}{(x(t))^2 + 1}. \end{aligned} \tag{2.3}$$

With positive initial condition $x(0) > 0$ and $y(0) > 0$. Here r is the per capita growth rate of the prey, β is the maximum value which per capita reduction rate of x can attain. The conversion rate of prey x into predator y is also considered to be β. System (2.3) *can be written in the form:*

$$F : \begin{pmatrix} x \\ y \end{pmatrix} \longmapsto \begin{pmatrix} rx\,(1-x) - \beta \dfrac{x^2 y}{x^2+1} \\ \beta \dfrac{x^2 y}{x^2+1} \end{pmatrix}. \tag{2.4}$$

3. Fixed Points: Existence and Stability

In this section, we look at the existence and stability of the system's fixed points in $\mathbb{R}^2_+$. Results about the existence of fixed points are summarized as follows:

Proposition 3.1. *For model* (2.4)*, we can have at most three fixed points:*

(i) *The trivial fixed point $E_0(0,0)$ always exists;*

(ii) *The predator-free fixed point $E_1\left(\frac{r-1}{r}, 0\right)$ exists if $r > 1$;*

(iii) *The interior fixed $E_2\left(\frac{1}{\sqrt{\beta-1}}, \frac{-r\sqrt{\beta-1}+(\beta-1)(r-1)}{(\beta-1)^{3/2}}\right)$ exists if $\beta > 2$ and $r > \frac{1-\beta}{\sqrt{\beta-1}-\beta+1}$.*

Proof. By solving the following algebraic system, the fixed points correspond to the steady states of the model population (2.4) can be obtained

$$\begin{aligned} rx\,(1-x) - \beta \frac{(x)^2 y}{(x)^2+1} - x &= 0, \\ \beta \frac{(x)^2 y}{(x)^2+1} - y &= 0, \end{aligned}$$

then all non-negative fixed points of the system (2.4) are $E_0(0,0)$, $E_1\left(\frac{r-1}{r}, 0\right)$, which is positive if $r > 1$ and $E_2\left(\frac{1}{\sqrt{\beta-1}}, \frac{(\beta-1)(r-1)-r\sqrt{\beta-1}}{(\beta-1)^{3/2}}\right)$, which is positive if $\beta > 2$ and $r > \frac{1-\beta}{\sqrt{\beta-1}-\beta+1}$. □

3.1. Dynamic Behavior of the Model

Now, we will investigate how the solutions of model (2.4) behave around E_0, E_1, and E_2. Computing the variation matrix corresponding to each fixed point can be used to study model (2.4) local stability. The Jacobian matrix of model (2.4) $J(x,y)$ about the fixed point (x,y) is provided by

$$J(x,y) = \begin{pmatrix} r(1-x) - rx - \dfrac{2\beta xy}{x^2+1} + \dfrac{2\beta x^3 y}{(x^2+1)^2} & -\dfrac{\beta x^2}{x^2+1} \\ \dfrac{2\beta xy}{(x^2+1)^2} & \dfrac{\beta x^2}{x^2+1} \end{pmatrix},$$

its characteristic equation is

$$\lambda^2 - p(x,y)\lambda + q(x,y) = 0, \tag{3.1}$$

where

$$p(x,y) = \frac{-2rx^5 + (r+\beta)x^4 - 4rx^3 + (2r+\beta)x^2 - 2(\beta y + r)x + r}{(x^2+1)^2},$$

$$q(x,y) = \frac{\beta r x^2(1-2x)}{x^2+1},$$

we recall the following definitions:

Definition 3.1. Let $E(x,y)$ be a fixed point of (2.4) and let μ_1 and μ_2 are the eigenvalues of (3.1).

(i) E is called a sink (locally asymptotic stable) if $\mid \mu_1 \mid < 1$ and $\mid \mu_2 \mid < 1$;

(ii) E is called a source if $\mid \mu_1 \mid > 1$ and $\mid \mu_2 \mid > 1$. A source is locally unstable;

(iii) E is called a saddle if $\mid \mu_1 \mid < 1$ and $\mid \mu_2 \mid > 1$ (or $\mid \mu_1 \mid > 1$ and $\mid \mu_2 \mid < 1$);

(iv) E is called non-hyperbolic if either $\mid \mu_1 \mid = 1$ and $\mid \mu_2 \mid = 1$.

The relations between roots and coefficients of the quadratic equation is given by the following Lemma.

Lemma 3.1. *Let $R(\mu) = \mu^2 + A\mu + B$. Suppose that $R(1) > 0$, μ_1 and μ_2 are the roots of $R(\mu) = 0$. Then*

(i) $\mid \mu_1 \mid < 1$ *and* $\mid \mu_2 \mid < 1$ *if and only if* $R(-1) > 0$ *and* $B < 1$;

(ii) $\mid \mu_1 \mid < 1$ *and* $\mid \mu_2 \mid > 1$ *(or* $\mid \mu_1 \mid > 1$ *and* $\mid \mu_2 \mid < 1$*) if and only if* $R(-1) < 0$;

(iii) $\mid \mu_1 \mid > 1$ *and* $\mid \mu_2 \mid > 1$ *if and only if* $R(-1) > 0$ *and* $B > 1$;

(iv) $\mu_1 = -1$ *and* $\mid \mu_2 \mid \neq 1$ *if and only if* $R(-1) = 0$ *and* $B \neq 0, 2$;

(v) μ_1 *and* μ_2 *are complex and* $\mu_1 = \mid \mu_2 \mid = 1$ *if and only if* $A^2 - 4B < 0$ *and* $B = 1$. □

Under certain conditions, the following Proposition confirms the stability of the fixed points of the system (2.4).

Proposition 3.2. *For the fixed point E_0 of the system (2.4), the following statements are true:*

(i) E_0 *is sink if* $0 < r < 1$;

(ii) E_0 *is never a source;*

(iii) E_0 *is an unstable saddle if* $r > 1$;

(iv) E_0 *is non-hyperbolic if* $r = 1$.

Proof. The Jacobian matrix associated with (2.4) at E_0 is $J(E_0)$ and is given by

$$J(E_0) = \begin{pmatrix} r & 0 \\ 0 & 0 \end{pmatrix},$$

the eigenvalues of $J(E_0)$ are $\lambda_1 = 0$ and $\lambda_2 = r$. So, the fixed point

(i) E_0 is a sink if and only if $0 < r < 1$;

(ii) E_0 is never a source since one of the eigenvalues is always zero;

(iii) E_0 is a saddle if and only if $r > 1$;

(iv) E_0 is non-hyperbolic if only if $r = 1$.

□

Proposition 3.3. *The fixed point E_1 is asymptotically stable if and only if $1 < r < 3$ and $\beta < \frac{2r^2-2r+1}{(r-1)^2}$. Moreover, it loses stability:*

(i) *via branching for $r = 1$ and there bifurcates to E_0;*

(ii) *via branching for $\beta = \frac{2r^2-2r+1}{(r-1)^2}$ and there bifurcates to E_2 if $1 < r < 3$;*

(iii) *via a supercritical flip for $r = 3$ and $\beta < \frac{13}{4}$.*

Proof. The Jacobian matrix of (2.4) at E_1 is given by

$$J(E_1) = \begin{pmatrix} 2-r & -\dfrac{\beta(r-1)^2}{2r^2-2r+1} \\ 0 & \dfrac{\beta(r-1)^2}{2r^2-2r+1} \end{pmatrix}, \tag{3.2}$$

the eigenvalues of $J(E_1)$ are $\lambda_1 = 2 - r$ and $\lambda_2 = \frac{\beta(r-1)^2}{2r^2-2r+1}$. The fixed point E_1 is asymptotically stable if and only if $|\lambda_1| < 1$ and $|\lambda_2| < 1$, that is, if and only if $1 < r < 3$ and $\beta < \frac{2r^2-2r+1}{(r-1)^2}$.

The stability region's boundary points must meet one of three conditions:
(i) $r = 1$,
(ii) $r = 3$,
(iii) $\beta = \frac{2r^2-2r+1}{(r-1)^2}$,
in the first case, according to Proposition 3.2 E_0 is stable if $0 < r < 1$, and loses its stability at $r = 1$. In (r, x)-space E_0 forms the curve $(r, 0)$ with tangent vector $(1, 0)$. E_1 is represented in (r, x)-space by the curve $(r, \frac{r-1}{r})$. When $r = 1$, these curves intersect at $(1, 0)$ and the tangent vector in (r, x)-space is $(1, 1)$, so it is clear that E_0 branches to E_1 for $r = 1$.

In the second case, this is a stability boundary only if $1 < r < 3$. The Jacobian (3.2) then has an eigenvalue $+1$, and these boundary points are also E_2 points, which may be easily verified.

In the third case, this is a stability boundary only if $\beta < \frac{13}{4}$. In this case, $\lambda_1 = -1$ which means that E_1 loses stability via a period doubling point. It is sufficient to prove that the corresponding critical normal form coefficient b_1, determined via center manifold reduction, is positive for supercriticality of the period doubling point; see [26], Ch. 8 and [27].

$$b_1 = \frac{1}{6}\left\langle p, C(q,q,q) + 3B\left(q, (I-A)^{-1}B(q,q)\right)\right\rangle.$$

Here, $A = J(E_1)$, and $B(\cdot,\cdot), C(\cdot,\cdot,\cdot)$ are the second- and third- order multilinear forms, respectively, and p and q are the left and right eigenvectors of A for the eigenvalue -1, respectively. These vectors are normalized by $\langle p, q\rangle = 1, \langle q, q\rangle = 1$, where $\langle\cdot,\cdot\rangle$ is the standard scalar product in $\mathbb{R}^2$. We obtain

$$q = \begin{pmatrix} q_1 \\ q_2 \end{pmatrix} = \begin{pmatrix} 1 \\ 0 \end{pmatrix},$$

$$p = \begin{pmatrix} p_1 \\ p_2 \end{pmatrix} = \begin{pmatrix} 1 \\ \frac{4\beta}{13+4\beta} \end{pmatrix},$$

the components of the second-order multilinear form $B(q,q)$ are given by

$$[B(q,q)]_1 = \sum_{j,k=1}^{2} \frac{\partial^2 (rx\,(1-x) - \beta \frac{x^2 y}{x^2+1})}{\partial x_j \partial x_k} q_j q_k = -2r q_1 q_1 + \frac{108\beta}{169} q_2 q_2 = -6,$$

$$[B(q,q)]_2 = \sum_{j,k=1}^{2} \frac{\partial^2 (\beta \frac{x^2 y}{x^2+1})}{\partial x_j \partial x_k} q_j q_k = -\frac{108\beta}{169} q_1 q_2 = 0,$$

where the state variable vector is for ease of notation generically denoted by $(x_1, x_2)^T$ instead of $(x, y)^T$. Let $\eta = (I - A)^{-1} B(q,q)$, then we have $\eta = \begin{pmatrix} -3 \\ 0 \end{pmatrix}$ and find

$$B(q,\eta) = \begin{pmatrix} 18 \\ 0 \end{pmatrix},$$

the component of the third-order multilinear form $C(q,q,q)$ are given by

$$C(q,q,q) = \begin{pmatrix} 0 \\ 0 \end{pmatrix},$$

the critical normal form coefficient b_1 is given by

$$b_1 = \frac{1}{6} p^T \begin{pmatrix} 54 \\ 0 \end{pmatrix} = 9,$$

which is obviously positive. This completes the proving of the flip point's super-criticality E_1. □

The dynamical behavior of the system near the interior fixed point E_2 is of particular interest to us because of its significance. The Lemma (3.1) can be used to find conditions that guarantee that the characteristic roots of Jacobian matrices about E_2 are contained within the unit disc.

Proposition 3.4. *The positive equilibrium point E_2 of the discrete-time model* (2.4) *is locally asymptotically stable if and only if the following conditions holds*

(i) $r < \dfrac{(2\beta-1)\sqrt{\beta-1}}{-\sqrt{\beta-1}+\beta+1}$;

(ii) $r > \dfrac{\sqrt{\beta-1}}{\sqrt{\beta-1}-1}$;

(iii) $r(\sqrt{\beta-1}-2) < \sqrt{\beta-1}$.

Proof. The Jacobian matrix of (2.4) at E_2 is given by

$$J(E_2) = \begin{pmatrix} -\dfrac{((r-2)\beta - 2r + 2)\sqrt{\beta-1} + 2r}{\sqrt{\beta-1}\beta} & -1 \\ \dfrac{-2r\sqrt{\beta-1} + 2(\beta-1)(r-1)}{\beta} & 1 \end{pmatrix},$$

and the characteristic equation of $J(E_2)$ is

$$\lambda^2 - p\lambda + q = 0,$$

where

$$p = -\frac{((r-3)\beta - 2r + 2)\sqrt{\beta-1} + 2r}{\beta\sqrt{\beta-1}},$$
$$q = \frac{r(\sqrt{\beta-1} - 2)}{\sqrt{\beta-1}},$$

according to lemma (3.1), the positive equilibrium point E_2 is locally asymptotically stable if

$$|p| < 1 + q < 2.$$

We note that the the criterion $1 + p + q > 0$ is easily seen to be equivalent to the condition

$$r < \frac{(2\beta-1)\sqrt{\beta-1}}{-\sqrt{\beta-1} + \beta + 1},$$

next, the criterion $1 - p + q > 0$ is easily seen to be equivalent to

$$r > \frac{\sqrt{\beta-1}}{\sqrt{\beta-1} - 1},$$

the criterion $1 - q > 0$ translates as

$$r(\sqrt{\beta-1} - 2) < \sqrt{\beta-1}.$$

□

The three curves $r = \frac{(2\beta-1)\sqrt{\beta-1}}{-\sqrt{\beta-1}+\beta+1}$, $r = \frac{\sqrt{\beta-1}}{\sqrt{\beta-1}-1}$, and $r = \frac{\sqrt{\beta-1}}{\sqrt{\beta-1}-2}$ are forming boundaries for the stability region of fixed point E_2 (see Figure 1). The curves $r = \frac{(2\beta-1)\sqrt{\beta-1}}{-\sqrt{\beta-1}+\beta+1}$ and $r = \frac{\sqrt{\beta-1}}{\sqrt{\beta-1}-1}$ intersect solely at $D_1(r = 3, \beta = \frac{13}{4})$, and the curves $r = \frac{(2\beta-1)\sqrt{\beta-1}}{-\sqrt{\beta-1}+\beta+1}$ and $r = \frac{\sqrt{\beta-1}}{\sqrt{\beta-1}-2}$ meet at $D_2(r \approx 5.678685656, \beta \approx 6.892551992)$.

The case of the nonhyperbolic fixed point is more complicated. There are various possible possibilities based on eigenvalues of 1 or -1. When one of the eigenvalues is in the unit circle and the other eigenvalue is inside the unit circle, it's customary to apply center manifold theory to determine the stability of the fixed point [10,26,31].

Proposition 3.5. *E_2 loses stability:*

(i) *via a flip point when $\frac{13}{4} < \beta < 6.892551992$ and $r = \frac{(2\beta-1)\sqrt{\beta-1}}{-\sqrt{\beta-1}+\beta+1}$;*

(ii) *via a Neimark-Sacker point when $6.892551992 < \beta$ and $r = \frac{\sqrt{\beta-1}}{\sqrt{\beta-1}-2}$;*

(iii) *via a branch point when $\frac{13}{4} < \beta$ and $r = \frac{\sqrt{\beta-1}}{\sqrt{\beta-1}-1}$ where it bifurcates to E_1;*

(iv) *via a branch-flip (BPPD) point at $D_1(r = 3, \beta = \frac{13}{4})$;*

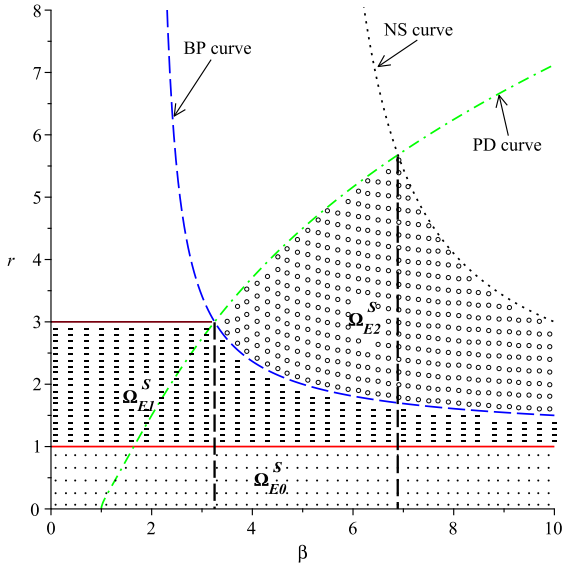

Figure 1. Stability regions in (β, r)-space.

(v) *via a resonance 1: 2 point at* $D_2(r \approx 5.678685656, \beta \approx 6.892551992)$.

Proof. The stability boundary of E_2, according to Proposition 3.4, is made up of sections of three curves, namely,
(1) Curve 1: $r = \frac{(2\beta-1)\sqrt{\beta-1}}{-\sqrt{\beta-1}+\beta+1}$,
(2) Curve 2: $r = \frac{\sqrt{\beta-1}}{\sqrt{\beta-1}-1}$,
(3) Curve 3: $r = \frac{\sqrt{\beta-1}}{\sqrt{\beta-1}-2}$.

On the stability boundary of E_2, the points of Curve 1 meet $1 + p + q = 0$, meaning that they have an eigenvalue of -1 and, thus, are period doubling points. The points of Curve 3 which are on the stability boundary satisfy $q = 1$, that is, they have two eigenvalues with product 1, and, thus, are Neimark-Sacker points. On the stability boundary, the points of Curve 2 satisfy $1-p+q = 0$, meaning that they have an eigenvalue of 1. It's straightforward to see that E_2 then branches to E_1.

When this is combined with Proposition 3.3, the interior points of the boundary parts of Curves 1,2, and 3 create the sets specified in this Proposition parts (i), (ii), and (iii), respectively.

When $r = 3$ and $\beta = \frac{13}{4}$ the intersection point of Curves 1 and 2 is a branch flip point (BPPD) with eigenvalues -1 and 1. The intersection point of Curves 1 and 3 (when $r \approx 5.678685656$ and $\beta \approx 6.892551992$) is a resonance $1 : 2$ point with double eigenvalue -1. □

4. Bifurcations analysis

The bifurcation analysis of model (2.4) is the focus of this section. The number of fixed points and their topological types change as the parameters (r, β) vary in

different regions, according to the results in Propositions 3.4 and 3.5.

4.1. Neimark–Sacker bifurcation about E_2

Firstly, we will discuss the Neimark-Sacker bifurcation of the discrete-time model (2.4) about E_2. Consider the parameter r in a neighborhood of r^*, i.e., $r = r^* + \epsilon$ where $\epsilon \ll 1$, then the discrete-time model (2.4) becomes

$$\begin{aligned} x_{n+1} &= (r^* + \epsilon)\, x_n\,(1 - x_n) - \beta \frac{x_n^2 y_n}{x_n^2 + 1}, \\ y_{n+1} &= \beta \frac{x_n^2 y_n}{x_n^2 + 1}. \end{aligned} \tag{4.1}$$

The characteristic equation of $J_{E_2}\Big(\frac{1}{\sqrt{\beta-1}}, \frac{-(r^*+\epsilon)\sqrt{\beta-1}+(\beta-1)(r^*+\epsilon-1)}{(\beta-1)^{3/2}}\Big)$ of the discrete-time model (4.1) about $E_2\left(\frac{1}{\sqrt{\beta-1}}, \frac{-(r^*+\epsilon)\sqrt{\beta-1}+(\beta-1)(r^*+\epsilon-1)}{(\beta-1)^{3/2}}\right)$ is

$$\lambda^2 - p(\epsilon)\lambda + q(\epsilon) = 0,$$

where

$$\begin{aligned} p(\epsilon) &= -\frac{((r^* + \epsilon - 3)\beta - 2\,(r^* + \epsilon) + 2)\sqrt{\beta - 1} + 2\,(r^* + \epsilon)}{\sqrt{\beta - 1}\beta}, \\ q(\epsilon) &= \frac{(\sqrt{\beta - 1} - 2)\,(r^* + \epsilon)}{\sqrt{\beta - 1}}. \end{aligned}$$

The roots of characteristic equation of $J(E_2)$ are

$$\begin{aligned} \lambda_{1,2} &= \frac{p(\epsilon) \pm \iota\sqrt{4q(\epsilon) - p^2(\epsilon)}}{2}, \\ &= -\frac{((r^* + \epsilon - 3)\beta - 2r^* - 2\epsilon + 2)\sqrt{\beta - 1} + 2r^* + 2\epsilon}{2\beta\sqrt{\beta - 1}} \\ &\quad \pm \frac{\iota}{2}\sqrt{\frac{4(\sqrt{\beta-1}-2)(r^*+\epsilon)}{\sqrt{\beta-1}} - \frac{(((r^*+\epsilon-3)\beta-2r^*-2\epsilon+2)\sqrt{\beta-1}+2r^*+2\epsilon)^2}{(\beta-1)\beta^2}}, \\ |\lambda_{1,2}| &= \sqrt{q(\epsilon)} = \sqrt{\frac{(\sqrt{\beta - 1} - 2)\,(r^* + \epsilon)}{\sqrt{\beta - 1}}}, \end{aligned}$$

and

$$\left.\frac{d\,|\lambda_{1,2}|}{d\epsilon}\right|_{\epsilon=0} = \frac{\sqrt{\sqrt{\beta - 1} - 2}}{2\sqrt{r}(\beta - 1)^{1/4}} > 0.$$

Additionally, we required that when $\epsilon = 0, \lambda_{1,2}^m \neq 1, m = 1, 2, 3, 4$, which corresponds to $p(0) \neq -2, 0, 1, 2$, which is true by computation.

Let $u_n = x_n - x^*, v_n = y_n - y^*$ then the equilibrium E_2 of the discrete-time model (2.4) transforms into $O(0, 0)$.

By manipulation, one gets

$$\begin{aligned} u_{n+1} &= (r^* + \epsilon)\,(u_n + x^*)\,(1 - u_n - x^*) - \frac{\beta\,(u_n + x^*)^2\,(v_n + y^*)}{(u_n + x^*)^2 + 1} - x^*, \\ v_{n+1} &= \frac{\beta\,(u_n + x^*)^2\,(v_n + y^*)}{(u_n + x^*)^2 + 1} - y^*, \end{aligned} \tag{4.2}$$

where $x^* = \frac{1}{\sqrt{\beta-1}}, y^* = \frac{-r\sqrt{\beta-1}+(\beta-1)(r-1)}{(\beta-1)^{3/2}}$. Hereafter, when $\epsilon = 0$, the normal form of system (4.2) is studied. Expanding (4.2) up to fourth order about $(u_n, v_n) = (0, 0)$ by Taylor series, we get

$$\left.\begin{aligned} u_{n+1} &= \Lambda_{11}u_n + \Lambda_{12}v_n + \Lambda_{13}u_n^2 + \Lambda_{14}u_nv_n + \Lambda_{15}u_n^3 + \Lambda_{16}u_n^2v_n + O(|u_n|,|v_n|)^4, \\ v_{n+1} &= \Lambda_{21}u_n + \Lambda_{22}v_n + \Lambda_{22}u_n^2 + \Lambda_{24}u_nv_n + \Lambda_{25}u_n^3 + \Lambda_{26}u_n^2v_n + O(|u_n|,|v_n|)^4, \end{aligned}\right\}$$

where

$$\begin{aligned}
&\Lambda_{11} = -\tfrac{\left(2r^*(x^*)^5 - r^*(x^*)^4 + 4r^*(x^*)^3 + 2\beta x^*y^* - 2r^*(x^*)^2 + 2r^*x^* - r^*\right)}{((x^*)^2+1)^2}, \quad \Lambda_{12} = -\tfrac{\beta(x^*)^2}{(x^*)^2+1}, \\
&\Lambda_{13} = \tfrac{\left(-r^*(x^*)^6 - 3r^*(x^*)^4 + 3\beta(x^*)^2y^* - 3r^*(x^*)^2 - \beta y^* - r^*\right)}{((x^*)^2+1)^3}, \quad \Lambda_{14} = -\tfrac{2\beta x^*}{((x^*)^2+1)^2}, \\
&\Lambda_{15} = -\tfrac{4\beta x^*y^*((x^*)^2-1)}{((x^*)^2+1)^4}, \quad \Lambda_{16} = \tfrac{\beta(3(x^*)^2-1)}{((x^*)^2+1)^3}, \\
&\Lambda_{21} = \tfrac{2\beta x^*y^*}{((x^*)^2+1)^2}, \quad \Lambda_{22} = \tfrac{\beta(x^*)^2}{(x^*)^2+1}, \quad \Lambda_{23} = -\tfrac{\beta y^*\left(3(x^*)^2-1\right)}{((x^*)^2+1)^3}, \quad \Lambda_{24} = \tfrac{2\beta x^*}{((x^*)^2+1)^2}, \\
&\Lambda_{25} = -\Lambda_{15}, \quad \Lambda_{26} = -\Lambda_{16}.
\end{aligned}$$

Now, let

$$\begin{aligned}
\eta &= -\frac{((r^*+\epsilon-3)\beta - 2r^* - 2\epsilon + 2)\sqrt{\beta-1} + 2r^* + 2\epsilon}{2\beta\sqrt{\beta-1}}, \\
\zeta &= \frac{1}{2}\sqrt{\frac{4(\sqrt{\beta-1}-2)(r^*+\epsilon)}{\sqrt{\beta-1}} - \frac{(((r^*+\epsilon-3)\beta - 2r^* - 2\epsilon + 2)\sqrt{\beta-1} + 2r^* + 2\epsilon)^2}{(\beta-1)\beta^2}},
\end{aligned}$$

and the invertible matrix T defined by

$$T = \begin{pmatrix} \Lambda_{12} & 0 \\ \eta - \Lambda_{11} & -\zeta \end{pmatrix}.$$

Using the following translation:

$$\begin{pmatrix} u_n \\ v_n \end{pmatrix} = \begin{pmatrix} \Lambda_{12} & 0 \\ \eta - \Lambda_{11} & -\zeta \end{pmatrix} \begin{pmatrix} X_n \\ Y_n \end{pmatrix},$$

(4.2) gives

$$\begin{pmatrix} X_{n+1} \\ Y_{n+1} \end{pmatrix} = \begin{pmatrix} \eta & -\zeta \\ \zeta & \eta \end{pmatrix} \begin{pmatrix} X_n \\ Y_n \end{pmatrix} + \begin{pmatrix} \Phi(X_n, Y_n) \\ \Psi(X_n, Y_n) \end{pmatrix}, \tag{4.3}$$

where

$$\begin{aligned}
\Phi(X_n, Y_n) &= \Pi_{11}{X_n}^2 + \Pi_{12}X_nY_n + \Pi_{13}X_n^3 + \Pi_{14}X_n^2Y_n + O(|X_n|,|Y_n|)^4, \\
\Psi(X_n, Y_n) &= \Pi_{21}{X_n}^2 + \Pi_{22}X_nY_n + \Pi_{23}X_n^3 + \Pi_{24}X_n^2Y_n + O(|X_n|,|Y_n|)^4,
\end{aligned}$$

and

$$\Pi_{11} = \Lambda_{12}\Lambda_{13} + \Lambda_{14}(\eta - \Lambda_{11}),$$

$$
\begin{aligned}
\Pi_{12} &= -\zeta\Lambda_{14},\\
\Pi_{13} &= \Lambda_{12}(\Lambda_{15}\Lambda_{12} + \Lambda_{16}(\eta - \Lambda_{11})),\\
\Pi_{14} &= -\zeta\Lambda_{16}\Lambda_{12},\\
\Pi_{21} &= \frac{1}{\zeta}\left[(\eta - \Lambda_{11})\left(\Lambda_{12}(\Lambda_{13} - \Lambda_{24}) + \Lambda_{14}(\eta - \Lambda_{11})\right) - \Lambda_{23}\Lambda_{12}^2\right],\\
\Pi_{22} &= \Lambda_{14}(\eta - \Lambda_{11}) - \Lambda_{24}\Lambda_{12},\\
\Pi_{23} &= \frac{\Lambda_{12}}{\zeta}\left[\Lambda_{16}\left(\eta - \Lambda_{11}\right)^2 - \Lambda_{25}\Lambda_{12}^2 - \left(\Lambda_{26} - \Lambda_{15}\right)\left(\eta - \Lambda_{11}\right)\Lambda_{12}\right],\\
\Pi_{24} &= \Lambda_{26}\Lambda_{12}^2 - \Lambda_{12}\Lambda_{16}\left(\eta - \Lambda_{11}\right).
\end{aligned}
$$

In addition,

$$
\begin{aligned}
&\Phi_{X_nX_n}|_{(0,0)} = 2\Pi_{11}, \quad \Phi_{X_nY_n}|_{(0,0)} = \Pi_{12}, \quad \Phi_{Y_nY_n}|_{(0,0)} = 0,\\
&\Phi_{X_nX_nX_n}|_{(0,0)} = 6\Pi_{13}, \quad \Phi_{X_nX_nY_n}|_{(0,0)} = 2\Pi_{14}, \quad \Phi_{X_nY_nY_n}|_{(0,0)} = \Phi_{Y_nY_nY_n}|_{(0,0)} = 0,
\end{aligned}
$$

and

$$
\begin{aligned}
&\Psi_{X_nX_n}|_{(0,0)} = 2\Pi_{21}, \quad \Psi_{X_nY_n}|_{(0,0)} = \Pi_{22}, \quad \Psi_{Y_nY_n}|_{(0,0)} = 0,\\
&\Psi_{X_nX_nX_n}|_{(0,0)} = 6\Pi_{23}, \quad \Psi_{X_nX_nY_n}|_{(0,0)} = 2\Pi_{24}, \quad \Psi_{X_nY_nY_n}|_{(0,0)} = \Psi_{Y_nY_nY_n}|_{(0,0)} = 0.
\end{aligned}
$$

In order for (4.3) to undergo a Neimark-Sacker bifurcation, it is mandatory that the following discriminatory quantity, i.e., $\chi \neq 0$ (see [10, 26, 28]),

$$
\chi = -\operatorname{Re}\left[\frac{(1-2\bar{\lambda})\bar{\lambda}^2}{1-\lambda}\tau_{11}\tau_{20}\right] - \frac{1}{2}\|\tau_{11}\|^2 - \|\tau_{02}\|^2 + \operatorname{Re}\left(\bar{\lambda}\tau_{21}\right),
$$

where

$$
\begin{aligned}
\tau_{02} &= \frac{1}{8}\left[\Phi_{X_nX_n} - \Phi_{Y_nY_n} + 2\Psi_{X_nY_n} + \iota\left(\Psi_{X_nX_n} - \Psi_{Y_nY_n} + 2\Phi_{X_nY_n}\right)\right]\Big|_{(0,0)},\\
\tau_{11} &= \frac{1}{4}\left[\Phi_{X_nX_n} + \Phi_{Y_nY_n} + \iota\left(\Psi_{X_nX_n} + \Psi_{Y_nY_n}\right)\right]\Big|_{(0,0)},\\
\tau_{20} &= \frac{1}{8}\left[\Phi_{X_nX_n} - \Phi_{Y_nY_n} + 2\Psi_{X_nY_n} + \iota\left(\Psi_{X_nX_n} - \Psi_{Y_nY_n} - 2\Phi_{X_nY_n}\right)\right]\Big|_{(0,0)},\\
\tau_{21} &= \frac{1}{16}\left[\Phi_{X_nX_nX_n} + \Phi_{X_nY_nY_n} + \Psi_{X_nX_nY_n} + \Psi_{Y_nY_nY_n}\right.\\
&\quad \left. + \iota\left(\Psi_{X_nX_nX_n} + \Psi_{X_nY_nY_n} - \Phi_{X_nX_nY_n} - \Phi_{Y_nY_nY_n}\right)\right]|_{(0,0)}.
\end{aligned}
$$

After calculating, we get

$$
\begin{aligned}
\tau_{02} &= \frac{1}{4}\left[\Pi_{11} + \Pi_{22} + \iota\left(\Pi_{21} + \Pi_{12}\right)\right],\\
\tau_{11} &= \frac{1}{2}\left[\Pi_{11} + \iota\Pi_{21}\right],\\
\tau_{20} &= \frac{1}{4}\left[\Pi_{11} + \Pi_{22} + \iota\left(\Pi_{21} - \Pi_{12}\right)\right],\\
\tau_{21} &= \frac{1}{8}\left[3\Pi_{23} + \Pi_{24} + \iota\left(3\Pi_{23} - \Pi_{24}\right)\right].
\end{aligned}
$$

Based on this analysis and the Neimark-Sacker bifurcation theorem discussed in [6, 16, 22, 26, 27], we arrive at the following Proposition.

Proposition 4.1. *If $\chi \neq 0$ then the discrete-time model (2.4) undergoes a Neimark-Sacker bifurcation about E_2 as (β, r) satisfy condition 2 in Proposition 3.5. Additionally, an attracting (resp. repelling) closed curve bifurcates from E_2 if $\chi < 0$ (resp. $\chi > 0$).*

Remark 4.1. According to bifurcation theory discussed in [27], the bifurcation is called a supercritical Neimark-Sacker bifurcation if the discriminatory quantity $\chi < 0$.

4.2. Period-doubling bifurcation

The period-doubling bifurcation of model (2.4) at E_2 is investigated here, when parameters vary in a small neighborhood of

$$P_{E_2} = \left\{ (\beta, r) : r = \frac{(2\beta - 1)\sqrt{\beta - 1}}{-\sqrt{\beta - 1} + \beta + 1} \quad \text{and} \quad \frac{13}{4} < \beta < 6.892551992 \right\}.$$

Select arbitrary parameters (β, r) from P_{E_2}. We consider the parameter r^* as a new dependent variable, and we can get

$$\begin{aligned} x_{n+1} &= (r + r^*)\, x_n\, (1 - x_n) - \beta \frac{x_n^2 y_n}{x_n^2 + 1}, \\ y_{n+1} &= \beta \frac{x_n^2 y_n}{x_n^2 + 1}. \end{aligned} \tag{4.4}$$

Let $u_n = x_n - x^*, v_n = y_n - y^*$ then the equilibrium E_2 of the discrete-time model (4.4) transforms into $O(0, 0)$.

By calculating we get

$$\begin{aligned} u_{n+1} &= \widehat{\Lambda_{11}} u_n + \widehat{\Lambda_{12}} v_n + \widehat{\Lambda_{13}} u_n^2 + \widehat{\Lambda_{14}} u_n v_n + \Upsilon_{01} u_n r^* + \Upsilon_{02} u_n^2 r^* + \widehat{\Lambda_{15}} u_n^3 \\ &\quad + \widehat{\Lambda_{16}} v_n u_n^2 + O\left(|u_n|, |r^*|\right)^4, \\ v_{n+1} &= \widehat{\Lambda_{21}} u_n + \widehat{\Lambda_{22}} v_n + \widehat{\Lambda_{23}} u_n^2 + \widehat{\Lambda_{24}} u_n v_n + \widehat{\Lambda_{25}} u_n^3 + \widehat{\Lambda_{26}} v_n u_n^2 \\ &\quad + O\left(|u_n|, |v_n|\right)^4, \end{aligned} \tag{4.5}$$

where

$$\widehat{\Lambda_{11}} = -\frac{\left(2r(x^*)^5 - r(x^*)^4 + 4r(x^*)^3 + 2\beta x^* y^* - 2r(x^*)^2 + 2r(x^*) - r\right)}{\left((x^*)^2 + 1\right)^2},$$

$$\widehat{\Lambda_{12}} = -\frac{\beta (x^*)^2}{(x^*)^2 + 1},$$

$$\widehat{\Lambda_{13}} = \frac{\left(-r(x^*)^6 - 3r(x^*)^4 + 3\beta (x^*)^2 y^* - 3r(x^*)^2 - \beta y^* - r\right)}{\left((x^*)^2 + 1\right)^3},$$

$$\widehat{\Lambda_{14}} = -\frac{2\beta x^*}{\left((x^*)^2 + 1\right)^2},\ \Upsilon_{01} = -(2x^* - 1),\ \Upsilon_{02} = -1,\ \widehat{\Lambda_{15}} = -\frac{4\beta x^* y^* \left((x^*)^2 - 1\right)}{\left((x^*)^2 + 1\right)^4},$$

$$\widehat{\Lambda_{16}} = \frac{\beta \left(3(x^*)^2 - 1\right)}{\left((x^*)^2 + 1\right)^3},\ \widehat{\Lambda_{21}} = \frac{2\beta x^* y^*}{\left((x^*)^2 + 1\right)^2},\quad \widehat{\Lambda_{22}} = \frac{\beta (x^*)^2}{(x^*)^2 + 1},$$

$$\widehat{\Lambda_{23}} = -\frac{\beta y^* \left(3(x^*)^2 - 1\right)}{\left((x^*)^2 + 1\right)^3},\ \widehat{\Lambda_{24}} = \frac{2\beta x^*}{\left((x^*)^2 + 1\right)^2},\ \widehat{\Lambda_{25}} = \frac{4\beta x^* y^* \left((x^*)^2 - 1\right)}{\left((x^*)^2 + 1\right)^4},$$

$$\widehat{\Lambda_{26}} = -\frac{\beta\left(3(x^*)^2-1\right)}{\left((x^*)^2+1\right)^3}.$$

Now, construct an invertible matrix T

$$T = \begin{pmatrix} \widehat{\Lambda_{12}} & \widehat{\Lambda_{12}}, \\ -1-\widehat{\Lambda_{11}} & \lambda_2-\widehat{\Lambda_{11}} \end{pmatrix},$$

and use the translation

$$\begin{pmatrix} u_n \\ v_n \end{pmatrix} = \begin{pmatrix} \widehat{\Lambda_{12}} & \widehat{\Lambda_{12}} \\ -1-\widehat{\Lambda_{11}} & \lambda_2-\widehat{\Lambda_{11}} \end{pmatrix} \begin{pmatrix} X_n \\ Y_n \end{pmatrix},$$

(4.5) gives

$$\begin{pmatrix} X_{n+1} \\ Y_{n+1} \end{pmatrix} = \begin{pmatrix} -1 & 0 \\ 0 & \lambda_2 \end{pmatrix} \begin{pmatrix} X_n \\ Y_n \end{pmatrix} + \begin{pmatrix} \widehat{\Phi}\left(u_n, v_n, r^*\right) \\ \widehat{\Psi}\left(u_n, v_n, r^*\right) \end{pmatrix}, \tag{4.6}$$

where

$$\begin{aligned}
&\widehat{\Phi}\left(u_n, v_n, r^*\right) \\
=&\frac{\widehat{\Lambda_{13}}\left(\lambda_2-\widehat{\Lambda_{11}}\right)-2\widehat{\Lambda_{23}}\widehat{\Lambda_{12}}}{\widehat{\Lambda_{12}}\left(1+\lambda_2\right)}u_n^2+\frac{\widehat{\Lambda_{14}}\left(\lambda_2-\widehat{\Lambda_{11}}\right)-2\widehat{\Lambda_{12}}\widehat{\Lambda_{24}}}{\widehat{\Lambda_{12}}\left(1+\lambda_2\right)}u_nv_n \\
&+\frac{\Upsilon_{01}\left(\lambda_2-\widehat{\Lambda_{11}}\right)}{\widehat{\Lambda_{12}}\left(1+\lambda_2\right)}u_nr^*+\frac{\Upsilon_{02}\left(\lambda_2-\widehat{\Lambda_{11}}\right)}{\widehat{\Lambda_{12}}\left(1+\lambda_2\right)}u_n^2r^*+\frac{\widehat{\Lambda_{15}}\left(\lambda_2-\widehat{\Lambda_{11}}\right)-2\widehat{\Lambda_{12}}\widehat{\Lambda_{25}}}{\widehat{\Lambda_{12}}\left(1+\lambda_2\right)}u_n^3 \\
&+\frac{\widehat{\Lambda_{16}}\left(\lambda_2-\widehat{\Lambda_{11}}\right)-2\widehat{\Lambda_{12}}\widehat{\Lambda_{26}}}{\widehat{\Lambda_{12}}\left(1+\lambda_2\right)}u_n^2v_n+O\left(\left|u_n\right|,\left|v_n\right|,\left|r^*\right|\right)^4, \\
&\widehat{\Psi}\left(u_n, v_n, r^*\right) \\
=&\frac{\widehat{\Lambda_{13}}\left(1+\widehat{\Lambda_{11}}\right)+\widehat{\Lambda_{12}}\widehat{\Lambda_{23}}}{\widehat{\Lambda_{12}}\left(1+\lambda_2\right)}u_n^2+\frac{\widehat{\Lambda_{14}}\left(1+\widehat{\Lambda_{11}}\right)+\widehat{\Lambda_{12}}\widehat{\Lambda_{24}}}{\widehat{\Lambda_{12}}\left(1+\lambda_2\right)}u_nv_n \\
&+\frac{\Upsilon_{01}\left(1+\widehat{\Lambda_{11}}\right)}{\widehat{\Lambda_{12}}\left(1+\lambda_2\right)}u_nr^*+\frac{\Upsilon_{02}\left(1+\widehat{\Lambda_{11}}\right)}{\widehat{\Lambda_{12}}\left(1+\lambda_2\right)}u_n^2r^*+\frac{\widehat{\Lambda_{15}}\left(1+\widehat{\Lambda_{11}}\right)+\widehat{\Lambda_{12}}\widehat{\Lambda_{25}}}{\widehat{\Lambda_{12}}\left(1+\lambda_2\right)}u_n^3 \\
&+\frac{\widehat{\Lambda_{16}}\left(1+\widehat{\Lambda_{11}}\right)+\widehat{\Lambda_{12}}\widehat{\Lambda_{26}}}{\widehat{\Lambda_{12}}\left(1+\lambda_2\right)}u_n^2v_n+O\left(\left|u_n\right|,\left|v_n\right|,\left|r^*\right|\right)^4. \\
&u_n^2=\widehat{\Lambda_{12}}^2\left(X_n^2+2X_nY_n+Y_n^2\right), \\
&u_nv_n=-\widehat{\Lambda_{12}}\left(1+\widehat{\Lambda_{11}}\right)X_n^2+\left(\widehat{\Lambda_{12}}\left(\lambda_2-\widehat{\Lambda_{11}}\right)-\widehat{\Lambda_{12}}\left(1+\widehat{\Lambda_{11}}\right)\right)X_nY_n \\
&\qquad+\widehat{\Lambda_{12}}\left(\lambda_2-\widehat{\Lambda_{11}}\right)Y_n^2, \\
&u_nr^*=\widehat{\Lambda_{12}}X_nr^*+\widehat{\Lambda_{12}}Y_nr^*,
\end{aligned}$$

$$u_n^2 r^* = \widehat{\Lambda_{12}}^2 \left(X_n^2 r^* + 2X_n Y_n r^* + Y_n^2 r^*\right).$$

Hereafter we determine the center manifold $W^c(0,0)$ of (4.6) about $(0,0)$ in a small neighborhood of r^* [5,26,27,32]. By center manifold theorem, there exists a center manifold $W^c(0,0)$ that can be represented as follows:

$$W^c(0,0) = \left\{(X_n, Y_n) : Y_n = c_0 r^* + c_1 X_n^2 + c_2 X_n r^* + c_3 (r^*)^2 + O\left(\left(|X_n|, |r^*|\right)^3\right)\right\},$$

where $O\left(\left(|X_n| + |r^*|\right)^3\right)$ is a function with order at least three in their variables (X_n, r^*), and

$$\begin{aligned}
c_0 &= 0,\\
c_1 &= \frac{-\widehat{\Lambda_{23}}\widehat{\Lambda_{12}}^2 + \left(1+\widehat{\Lambda_{11}}\right)\left[\widehat{\Lambda_{14}}\left(1+\widehat{\Lambda_{11}}\right) - \widehat{\Lambda_{12}}(\widehat{\Lambda_{13}} - \widehat{\Lambda_{24}})\right]}{\lambda_2^2 - 1},\\
c_2 &= -\frac{\Upsilon_{01}\left(1+\widehat{\Lambda_{11}}\right)}{(1+\lambda_2)^2},\\
c_3 &= 0.
\end{aligned}$$

Therefore, we consider the map (4.6) restricted to $W^c(0,0)$ as follows:

$$f(X_n) = -X_n + h_1 X_n^2 + h_2 X_n r^* + h_3 X_n^2 r^* + h_4 X_n (r^*)^2 + h_5 X_n^3 + O\left(\left(|X_n|, |r^*|\right)^4\right), \quad (4.7)$$

where

$$\begin{aligned}
h_1 &= \frac{1}{1+\lambda_2}\Big[\widehat{\Lambda_{11}}^2\widehat{\Lambda_{14}} + \left(\left(\widehat{\Lambda_{23}} - \widehat{\Lambda_{13}}\right)\widehat{\Lambda_{12}} - \widehat{\Lambda_{14}}(\lambda_2 - 1)\right)\widehat{\Lambda_{11}}\\
&\quad + \left(\lambda_2\widehat{\Lambda_{13}} + \widehat{\Lambda_{23}}\right)\widehat{\Lambda_{12}} - \lambda_2\widehat{\Lambda_{14}}\Big],\\
h_2 &= \frac{1}{1+\lambda_2}\left[\Upsilon_{01}\left(\lambda_2 - \widehat{\Lambda_{11}}\right)\right],\\
h_3 &= \frac{1}{(\lambda_2-1)(\lambda_2+1)^3}\Big[\Big(-\Lambda_{14}(1+\Lambda_{11})\lambda_2^3 + \big(-\Lambda_{23}\Lambda_{12}^2 - 3(\Lambda_{13}-\Lambda_{24})(1+\Lambda_{11})\Lambda_{12}\\
&\quad + 4\Lambda_{11}^2\Lambda_{14} + 7\Lambda_{11}\Lambda_{14} + 3\Lambda_{14}\big)\lambda_2^2 + \big((5\Lambda_{11}\Lambda_{23} + 3\Lambda_{23})\Lambda_{12}^2 + 3\big((\Lambda_{13} - \frac{5}{3}\Lambda_{24})\Lambda_{11}\\
&\quad + \frac{1}{3}\Lambda_{13} - \Lambda_{24}\big)(1+\Lambda_{11})\Lambda_{12} - 3\Lambda_{14}\Lambda_{11}(\Lambda_{11} + \frac{4}{3})(1+\Lambda_{11})\big)\lambda_2 + (-3\Lambda_{11}\Lambda_{23}\\
&\quad - 4\Lambda_{23})\Lambda_{12}^2 - \big((\Lambda_{13} - 3\Lambda_{24})\Lambda_{11} - 2\Lambda_{24}\big)(1+\Lambda_{11})\Lambda_{12} + \Lambda_{11}^2\Lambda_{14}(1+\Lambda_{11})\Big)\Upsilon_{01}\\
&\quad + \Upsilon_{02}\Lambda_{12}(\lambda_2 - 1)(\lambda_2 - \Lambda_{11})(\lambda_2 + 1)^2\Big],\\
h_4 &= \frac{\Upsilon_{01}^2\left(\lambda_2 - \widehat{\Lambda_{11}}\right)\left(1+\widehat{\Lambda_{11}}\right)}{\left(\lambda_2^2 - 1\right)(\lambda_2 + 1)},
\end{aligned}$$

$$
\begin{aligned}
h_5 =& \frac{1}{(\lambda_2-1)(\lambda_2+1)^2}\Big[4\Lambda_{12}^4\Lambda_{23}^2+\big(6(\Lambda_{13}-\frac{4}{3}\Lambda_{24})\Lambda_{23}\Lambda_{11}-2\lambda_2^2\Lambda_{25}-2\lambda_2\Lambda_{23}(\Lambda_{13}\\
&-\Lambda_{24})+4\Lambda_{13}\Lambda_{23}-6\Lambda_{23}\Lambda_{24}+2\Lambda_{25}\big)\Lambda_{12}^3+\Big(\big(-6\Lambda_{14}\Lambda_{23}+2(\Lambda_{13}-\Lambda_{24})(\Lambda_{13}\\
&-2\Lambda_{24})\big)\Lambda_{11}^2+\big((2\Lambda_{26}-\Lambda_{15})\lambda_2^2+\big(3\Lambda_{14}\Lambda_{23}-2(\Lambda_{13}-\Lambda_{24})^2\big)\lambda_2+2\Lambda_{13}^2-8\Lambda_{13}\Lambda_{24}\\
&-9\Lambda_{14}\Lambda_{23}+6\Lambda_{24}^2-2\Lambda_{26}+\Lambda_{15}\big)\Lambda_{11}+\lambda_2^3\Lambda_{15}+(2\Lambda_{26}-\Lambda_{14}\Lambda_{23})\lambda_2^2+4\Lambda_{13}\Lambda_{24}\\
&-2\Lambda_{13}^2+\Lambda_{14}\Lambda_{23}-2\Lambda_{24}^2-\Lambda_{15})\lambda_2-2\Lambda_{13}\Lambda_{24}-4\Lambda_{14}\Lambda_{23}+2\Lambda_{24}^2-2\Lambda_{26}\Big)\Lambda_{12}^2\\
&-(1+\Lambda_{11})\Big(4\Lambda_{14}(\Lambda_{13}-\frac{3}{2}\Lambda_{24})\Lambda_{11}^2+\big(\Lambda_{16}-\lambda_2^2\Lambda_{16}-5\lambda_2\Lambda_{14}(\Lambda_{13}-\Lambda_{24})\\
&+(3\Lambda_{13}-7\Lambda_{24})\Lambda_{14}+\Lambda_{16}\big)\Lambda_{11}+\lambda_2^3\Lambda_{16}+\Lambda_{14}(\Lambda_{13}-\Lambda_{24})\lambda_2^2+\big(3\Lambda_{14}(\Lambda_{24}-\Lambda_{13})\Lambda_{14}\\
&-\Lambda_{16}\big)\lambda_2-2\Lambda_{14}\Lambda_{24}\Big)\Lambda_{12}+\Lambda_{14}^2(1+\Lambda_{11})^2(\lambda_2-\Lambda_{11})(\lambda_2-2\Lambda_{11}-1)\Big].
\end{aligned}
$$

In order for the map (4.7) to undergo a period-doubling bifurcation, we require that the following discriminatory quantities are non-zero:

$$
\begin{aligned}
\Lambda_1 &= \left(\frac{\partial^2 f}{\partial X_n \partial r^*}+\frac{1}{2}\frac{\partial f}{\partial r^*}\frac{\partial^2 f}{\partial X_n^2}\right)\Big|_{(0,0)},\\
\Lambda_2 &= \left(\frac{1}{6}\frac{\partial^3 f}{\partial X_n^3}+\left(\frac{1}{2}\frac{\partial^2 f}{\partial X_n^2}\right)^2\right)\Big|_{(0,0)}.
\end{aligned}
$$

After calculating we obtain

$$\Lambda_1 = h_2+\frac{1}{2}h_3,$$

and

$$\Lambda_2 = h_5+h_1^2.$$

From the above analysis in [24] and theorem in [6,16,22,26,27],we have the following Proposition.

Proposition 4.2. *If $\Lambda_2 \neq 0$, the map (4.4) undergoes a period-doubling bifurcation about the unique positive equilibrium E_2 when r^* varies in a small neighborhood of $O(0,0)$. Moreover, if $\Lambda_2 > 0$ (resp $.\Lambda_2 < 0$), then the period-2 points that bifurcate from E_2 are stable (resp. unstable).*

5. Numerical simulations

In this section, we give some numerical simulations for model (2.4) to support our theoretical results. We will simulate the phase portraits of model (2.4) for different parameter regions. The MATLAB tool Cl MatContM will be used to perform a numerical bifurcation analysis; see [15, 27]. The bifurcation analysis is based on continuation methods, in which we trace solution manifolds of fixed points while changing some map parameters.

The bifurcation parameters are explored in the following four cases:

Case 1. Choosing $r = 0.5, \beta = 2$, with initial value $(x_0, y_0) = (0.1, 0.1)$, We see that model (2.4) has stable equilibrium point $E_0(0,0)$. Figure 2 shows the correctness of discussion about equilibrium $E_0 = (0,0)$ in Section 2. The MATCONTM

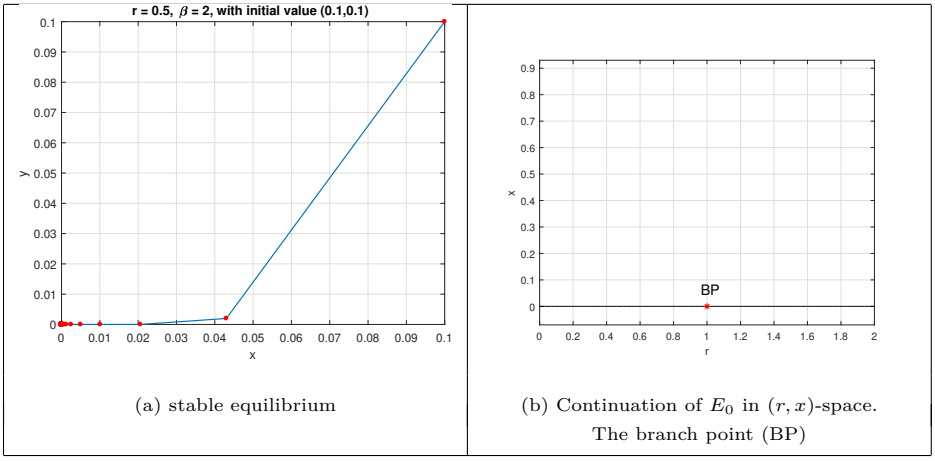

(a) stable equilibrium

(b) Continuation of E_0 in (r, x)-space. The branch point (BP)

Figure 2. Phase portrait of equilibrium point E_0 and its bifurcating to E_1

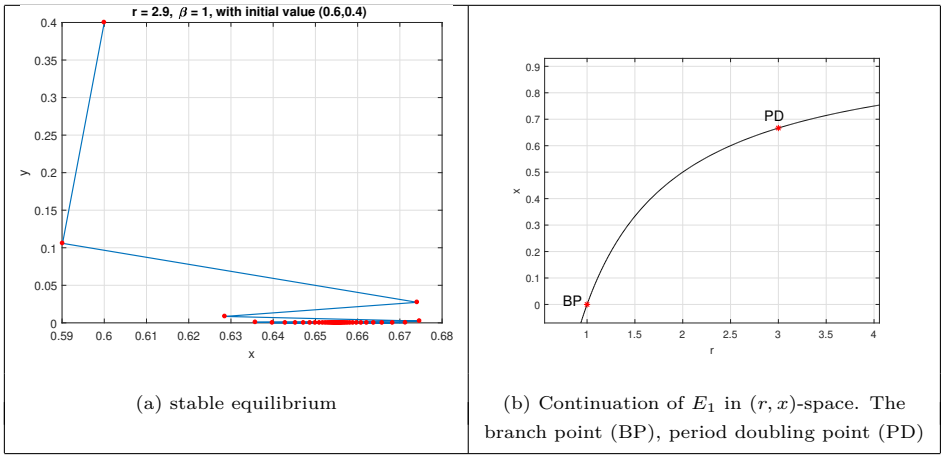

(a) stable equilibrium

(b) Continuation of E_1 in (r, x)-space. The branch point (BP), period doubling point (PD)

Figure 3. Phase portraits of equilibrium point E_1 and its bifurcation curve

report is

$$\text{label} = \text{BP}, \text{x} = \begin{pmatrix} 0.000000 & 0.000000 & 1.000000 \end{pmatrix},$$

From Figure 2 (b) we see that equilibrium $E_0 = (0, 0)$ loses its stability and bifurcates to E_1 when $r = 1$.

Case 2. Choosing $r = 2.9, \beta = 1$, with initial value $(x_0, y_0) = (0.6, 0.4)$, model (2.4) has stable equilibrium point $E_1(0.6551724138, 0)$. In stability region of E_1 with r free, we can see that E_1 is stable when $1 < r < 3$. It loses its stability via a supercritical period doubling point (PD) when $r = 3$, and via a branch point when $r = 1$ (see Figure 3 (b)). Figure 3 demonstrates the correctness of discussion about equilibrium $E_1\left(\frac{r-1}{r}, 0\right)$ in Section 2. The MATCONTM report is

$$\text{label} = \text{BP}, \text{x} = \begin{pmatrix} 0.000000 & 0.000000 & 1.000000 \end{pmatrix},$$

$$\text{label} = \text{PD}, \text{x} = \begin{pmatrix} 0.666667 & 0.000000 & 3.000000 \end{pmatrix},$$

Normal form coefficient of PD $= 2.700155e + 01$.

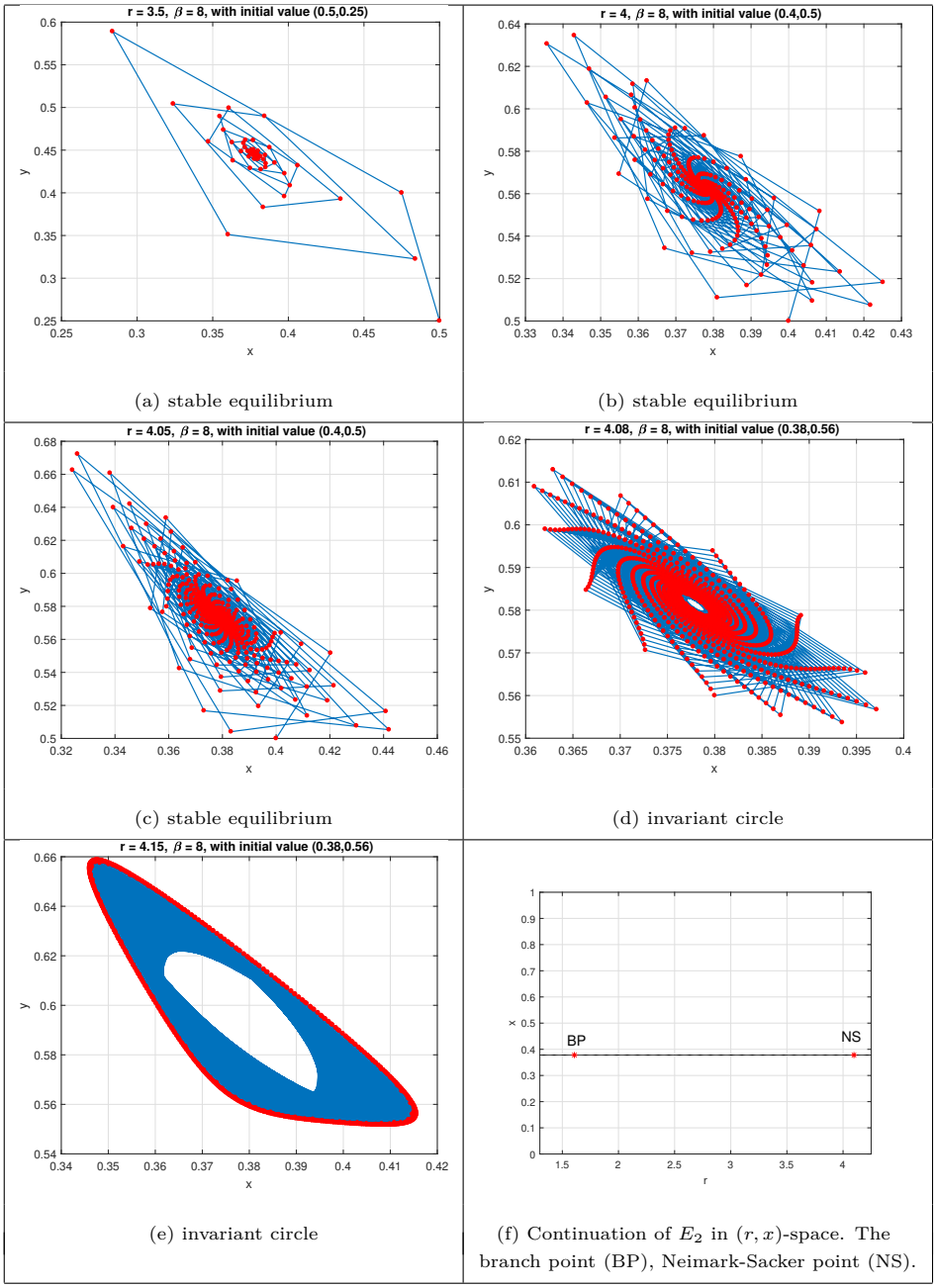

(a) stable equilibrium

(b) stable equilibrium

(c) stable equilibrium

(d) invariant circle

(e) invariant circle

(f) Continuation of E_2 in (r, x)-space. The branch point (BP), Neimark-Sacker point (NS).

Figure 4. Phase portraits of equilibrium point E_2 and its bifurcation curve

Case 3. Varying r in range $3.5 \leq r \leq 4.15$ and fixing $\beta = 8$. When $3.5 \leq r < 4.097167$ model (2.4) has a unique stable equilibrium point E_2, see Figure 4 (a-c).

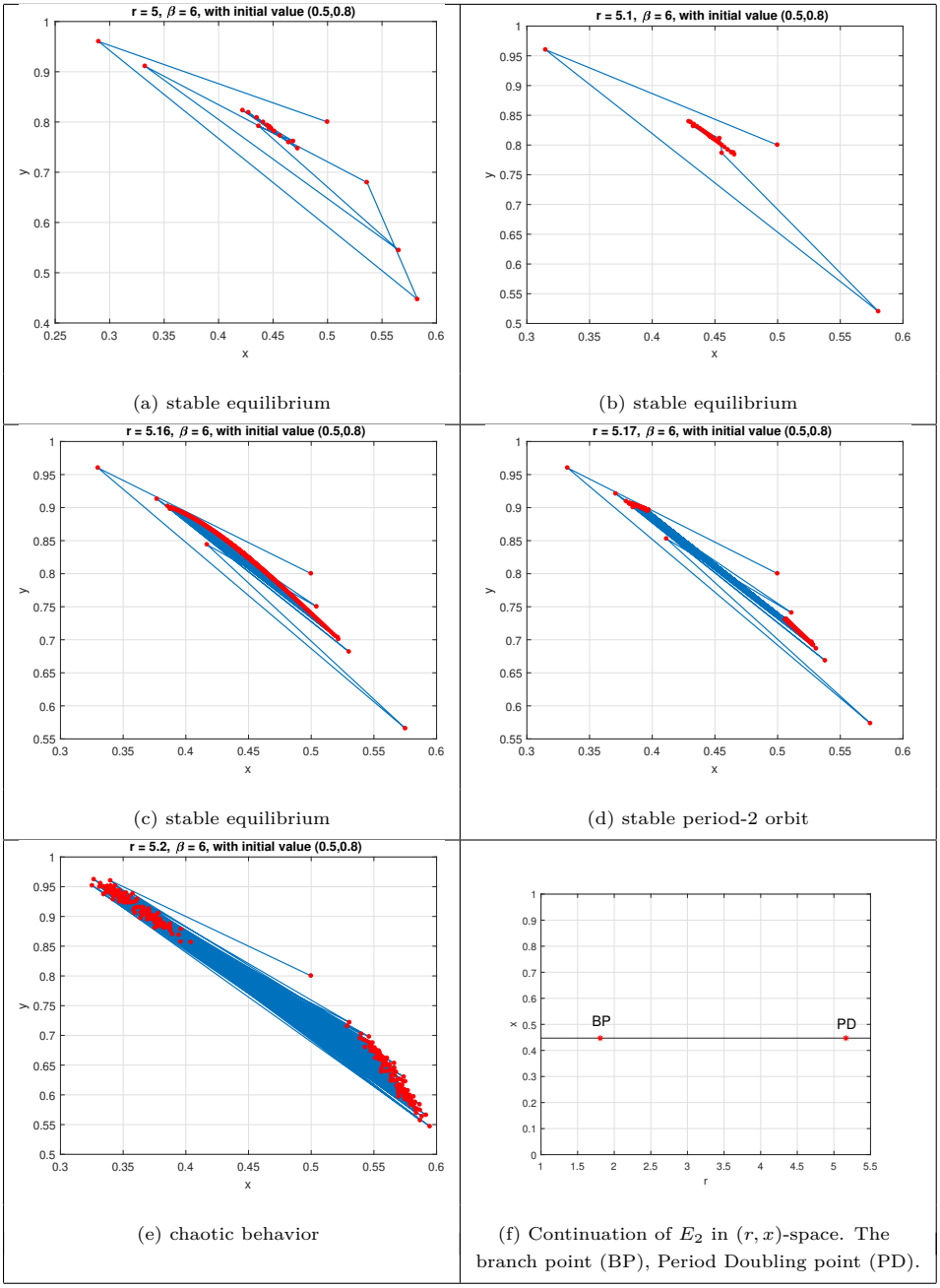

(a) stable equilibrium

(b) stable equilibrium

(c) stable equilibrium

(d) stable period-2 orbit

(e) chaotic behavior

(f) Continuation of E_2 in (r, x)-space. The branch point (BP), Period Doubling point (PD).

Figure 5. Phase portraits of equilibrium point E_2 and its bifurcation curve

E_2 loses its stability via a Neimark–Sacker bifurcation when $r = 4.097167$ with

$$\frac{\sqrt{\sqrt{\beta-1}-2}}{2\sqrt{r}(\beta-1)^{1/4}} = 0.1220355 > 0.$$

Moreover, the eigenvalues of J_{E_2} about E_2 are

$$\lambda_{1,2} = -0.3139822365 \pm 0.9368561103\iota, \tag{5.1}$$

after some calculations from Maple one gets

$$\begin{aligned} \tau_{02} &= 0.273120951 + 4.117649462\iota, \\ \tau_{11} &= -3.076368451 + 8.96217797\iota, \\ \tau_{20} &= 0.1365604746 + 2.42226425\iota, \\ \tau_{21} &= 3.628281910 - 21.18823279\iota. \end{aligned} \tag{5.2}$$

The value of the discriminatory quantity is $\chi = -58.79414975 < 0$ in light of (5.1) and (5.2). As a result, if $r > 4.097167$, the discrete-time model (2.4) undergoes a supercritical Neimark–Sacker bifurcation, resulting in a stable invariant close curve, as shown in Figure 4 (d-e). The MATCONTM report is

$$\begin{aligned} &\text{label} = \text{BP}, \text{x} = \begin{pmatrix} 0.377964 & 0.000000 & 1.607625 \end{pmatrix}, \\ &\text{label} = \text{NS}, \text{x} = \begin{pmatrix} 0.377964 & 0.585310 & 4.097167 \end{pmatrix}, \\ &\text{Normal form coefficient of NS} = -1.905451\text{e} + 01. \end{aligned}$$

Case 4. Varying r in range $5 \leq r \leq 5.2$ and fixing $\beta = 6$, with initial value $(x_0, y_0) = (0.5, 0.8)$. Figure 5 shows that equilibrium E_2 is stable for $r < 5.163119$, and loses its stability when $r = 5.163119$ via a period doubling bifurcation. Further, when $r > 5.163119$ a chaotic set is emerged with the increasing of r. The MATCONTM report is

$$\begin{aligned} &\text{label} = \text{BP}, \text{x} = \begin{pmatrix} 0.447214 & 0.000000 & 1.809017 \end{pmatrix}, \\ &\text{label} = \text{PD}, \text{x} = \begin{pmatrix} 0.447214 & 0.829180 & 5.163119 \end{pmatrix}, \\ &\text{Normal form coefficient of PD} = 3.336173\text{e} + 00. \end{aligned}$$

Algorithm analysis is the calculation of the amount of resources needed for an algorithm to be performed and the memory capacity provided by an algorithm. In this sense, parameters such as instruction space are regarded as constant in space complexity and parameters such as compile time. The running time of an algorithm is determined by the complexity of time and the complexity of space as a function. The amount of time needed for an algorithm to be performed is known as time complexity. Therefore, the time complexity of our algorithm is $O(n_k)$ where $1 \leq k$.

6. Conclusion

A planar map that models a predator-prey relationship with nonoverlapping generations was investigated in this study. Analytically, we were able to extract a detailed description of the stability regions of the system's fixed points, E_0, E_1, and E_2. Moreover, We used analytical methods, by direct computation of the normal form, to determine the criticality of the flip and Neimark-Sacker bifurcations for E_1

and E_2. In addition, system (2.4) exhibits a variety of dynamical behaviours that are interesting, such as an invariant cycle, a cascade of period-doubling, quasi-periodic orbits, and chaotic sets. This suggests that predators and prey can coexist in stable period-n orbits and an invariant cycle. These findings show that the discrete model has more richer dynamics than the continuous model.

References

[1] H. Agiza, E. ELabbasy, H. EL-Metwally and A. Elsadany, *Chaotic dynamics of a discrete prey–predator model with holling type II*, Nonlinear Analysis: Real World Applications, 2009, 10(1), 116–129.

[2] E. S. Allman and J. A. Rhodes, *Mathematical models in biology: an introduction*, Cambridge University Press, 2004.

[3] A. Almutairi, H. El-Metwally, M. Sohaly and I. Elbaz, *Lyapunov stability analysis for nonlinear delay systems under random effects and stochastic perturbations with applications in finance and ecology*, Advances in Difference Equations, 2021, 2021(1), 1–32.

[4] A. A. Berryman, *The orgins and evolution of predator-prey theory*, Ecology, 1992, 73(5), 1530–1535.

[5] J. Carr, *Applications of centre manifold theory*, Springer Science & Business Media, 2012, 35.

[6] J. D. Crawford, *Introduction to bifurcation theory*, Reviews of Modern Physics, 1991, 63(4), 991.

[7] Q. Din, *Complexity and chaos control in a discrete-time prey-predator model*, Communications in Nonlinear Science and Numerical Simulation, 2017, 49, 113–134.

[8] L. Edelstein-Keshet, *Mathematical models in biology*, SIAM, 2005.

[9] H. El-Metwally, M. Sohaly and I. Elbaz, *Mean-square stability of the zero equilibrium of the nonlinear delay differential equation: Nicholson's blowflies application*, Nonlinear Dynamics, 2021, 105(2), 1713–1722.

[10] S. N. Elaydi, *Discrete chaos: with applications in science and engineering*, Chapman and Hall/CRC, 2007.

[11] A.-E. A. Elsadany, H. El-Metwally, E. Elabbasy and H. Agiza, *Chaos and bifurcation of a nonlinear discrete prey-predator system*, Computational Ecology and Software, 2012, 2(3), 169.

[12] Q. Fang and X. Li, *Complex dynamics of a discrete predator–prey system with a strong allee effect on the prey and a ratio-dependent functional response*, Advances in Difference Equations, 2018, 2018(1), 1–16.

[13] H. Freedman, *A model of predator-prey dynamics as modified by the action of a parasite*, Mathematical biosciences, 1990, 99(2), 143–155.

[14] S. Gao and L. Chen, *The effect of seasonal harvesting on a single-species discrete population model with stage structure and birth pulses*, Chaos, Solitons & Fractals, 2005, 24(4), 1013–1023.

[15] W. Govaerts, Y. A. Kuznetsov, R. K. Ghaziani and H. Meijer, *Cl matcontm: A toolbox for continuation and bifurcation of cycles of maps*, Universiteit Gent, Belgium, and Utrecht University, The Netherlands, 2008.

[16] J. Guckenheimer and P. Holmes, *Nonlinear oscillations, dynamical systems, and bifurcations of vector fields*, Springer Science & Business Media, 2013, 42.

[17] M. Y. Hamada, T. El-Azab and H. El-Metwally, *Allee effect in a ricker type predator-prey model*, Journal of Mathematics and Computer Science, 2022, 29(03), 239–251.

[18] M. Y. Hamada, T. El-Azab and H. El-Metwally, *Bifurcation analysis of a two-dimensional discrete-time predator–prey model*, Mathematical Methods in the Applied Sciences, 2023, 46(4), 4815–4833.

[19] M. Y. Hamada, T. El-Azab and H. El-Metwally, *Bifurcations and dynamics of a discrete predator–prey model of ricker type*, Journal of Applied Mathematics and Computing, 2022, 69(1), 113–135.

[20] H. El-Metwally, AQ. Khan and M. Y. Hamada, *Allee effect in a Ricker type discrete-time predator–prey model with Holling type-II functional response*, Journal of Biological Systems, 2023, 31(2), 1–20.

[21] F. C. Hoppensteadt, *Mathematical methods of population biology*, Cambridge University Press, 1982, 4.

[22] G. Iooss, *Bifurcation of maps and applications*, Elsevier, 1979.

[23] F. Kangalgil and S. Kartal, *Stability and bifurcation analysis in a host–parasitoid model with hassell growth function*, Advances in Difference Equations, 2018, 2018(1), 1–15.

[24] A. Q. Khan, *Bifurcations of a two-dimensional discrete-time predator–prey model*, Advances in Difference Equations, 2019, 2019(1), 1–23.

[25] A. Q. Khan and H. El-Metwally, *Global dynamics, boundedness, and semicycle analysis of a difference equation*, Discrete Dynamics in Nature and Society, 2021, 2021, 1–10.

[26] Y. A. Kuznetsov, *Elements of applied bifurcation theory*, Springer-Verlag, New York, 2004, 112.

[27] Y. A. Kuznetsov and H. G. E. Meijer, *Numerical Bifurcation Analysis of Maps: From Theory to Software*, Cambridge University Press, 2019.

[28] X. Liu and D. Xiao, *Complex dynamic behaviors of a discrete-time predator–prey system*, Chaos, Solitons & Fractals, 2007, 32(1), 80–94.

[29] J. D. Murray, *Mathematical biology: I. an introduction. interdisciplinary applied mathematics*, Mathematical Biology, Springer, 2002.

[30] J. M. Smith and M. Slatkin, *The stability of predator-prey systems*, Ecology, 1973, 54(2), 384–391.

[31] S. Wiggins and M. Golubitsky, *Introduction to applied nonlinear dynamical systems and chaos*, Springer, 1990, 2.

[32] W. Zhang, *Discrete dynamical systems, bifurcations and chaos in economics*, elsevier, 2006.

[33] J. Zhao and Y. Yan, *Stability and bifurcation analysis of a discrete predator–prey system with modified holling–tanner functional response*, Advances in Difference Equations, 2018, 2018(1), 1–18.